Measurements and modeling of surface–atmosphere exchange of microorganisms in Mediterranean grassland

Federico Carotenuto, Teodoro Georgiadis, Beniamino Gioli, Christel Leyronas, Cindy E. Morris, Marianna Nardino, Georg Wohlfahrt, Franco Miglietta

Atmos. Chem. Phys., 17, 14919–14936, 2017
https://doi.org/10.5194/acp-17-14919-2017

Atmospheric Chemistry and Physics
Open Access
EGU

Measurements and modeling of surface–atmosphere exchange of microorganisms in Mediterranean grassland

Federico Carotenuto[1,2], Teodoro Georgiadis[2], Beniamino Gioli[2], Christel Leyronas[3], Cindy E. Morris[3], Marianna Nardino[2], Georg Wohlfahrt[1], and Franco Miglietta[2,4,5]

[1]Institute of Ecology, University of Innsbruck, Sternwartestrasse 15, Innsbruck, 6020, Austria
[2]Institute of Biometeorology (IBIMET), Consiglio Nazionale delle Ricerche (CNR), Via G. Caproni 8, 50145, Florence, Italy
[3]Plant Pathology Research Unit, French National Institute for Agricultural Research (INRA), Allée des Chênes 67, Montfavet, 84143, France
[4]FoxLab, Joint Research Unit Fondazione Edmund Mach – CNR IBIMET, Via E. Mach 1, San Michele all'Adige, 38010, Italy
[5]IMèRA, Universitè Aix-Marseille 2, Place le Verrier, Marseille, 13004, France

Correspondence: Federico Carotenuto (f.carotenuto@ibimet.cnr.it)

Received: 6 June 2017 – Discussion started: 14 June 2017
Revised: 5 October 2017 – Accepted: 7 November 2017 – Published: 18 December 2017

Abstract. Microbial aerosols (mainly composed of bacterial and fungal cells) may constitute up to 74 % of the total aerosol volume. These biological aerosols are not only relevant to the dispersion of pathogens, but they also have geochemical implications. Some bacteria and fungi may, in fact, serve as cloud condensation or ice nuclei, potentially affecting cloud formation and precipitation and are active at higher temperatures compared to their inorganic counterparts. Simulations of the impact of microbial aerosols on climate are still hindered by the lack of information regarding their emissions from ground sources. This present work tackles this knowledge gap by (i) applying a rigorous micrometeorological approach to the estimation of microbial net fluxes above a Mediterranean grassland and (ii) developing a deterministic model (the PLAnET model) to estimate these emissions on the basis of a few meteorological parameters that are easy to obtain. The grassland is characterized by an abundance of positive net microbial fluxes and the model proves to be a promising tool capable of capturing the day-to-day variability in microbial fluxes with a relatively small bias and sufficient accuracy. PLAnET is still in its infancy and will benefit from future campaigns extending the available training dataset as well as the inclusion of ever more complex and critical phenomena triggering the emission of microbial aerosol (such as rainfall). The model itself is also adaptable as an emission module for dispersion and chemical transport models, allowing further exploration of the impact of land-cover-driven microbial aerosols on the atmosphere and climate.

1 Introduction

Vegetated land surfaces, and plant leaves in particular, harbor a large number of microorganisms that can be transported by wind. It has been estimated that the planetary phyllosphere harbors about 10^{24} to 10^{26} bacterial cells (Morris et al., 2002) of the 10^{30} that live on Earth (Whitman et al., 1998). Up to 10^{7} bacteria per square centimeter are present on leaf surfaces (Morris et al., 2004), and plant materials are considered the largest source of fungal spores in the atmosphere (Burge, 2002). All of these organisms can be transported into the atmosphere by wind (Delort et al., 2010), as was shown experimentally in an artificial wind gust chamber (Lighthart et al., 1993). Atmospheric transport can involve both multiple short-distance events (Brown and Hovmøller, 2002), as well as single long-range movements. The latter are well known to transport desert dust (Rosselli et al., 2015; Peter et al., 2014; Kellogg and Griffin, 2006; Griffin, 2007; Weil et al., 2017), while long-range transport of epiphytic organisms living in plant canopies is much less documented. Nevertheless, living and dead microorganisms are part of primary biolog-

ical aerosols (PBAs) that contribute 13 to 74 % of the entire aerosol volume globally (Graham et al., 2003). Furthermore, microorganisms can be found in cloud water droplets. Water sampled from clouds over alpine regions in France and Austria contained about 2×10^4 mL^{-1} of bacteria (Amato et al., 2007; Bauer et al., 2003), while fungi were at least an order of magnitude lower. Different bacterial species were also found in fog droplets of the Po Plain in Italy (Fuzzi et al., 1997), as well as in clouds over Scotland (Ahern et al., 2007).

The presence of microorganisms in the atmosphere may be relevant to climate processes given that some of these microorganisms can serve as cloud condensation or ice nuclei (Möhler et al., 2007; Morris et al., 2004; Szyrmer and Zawadzki, 1997; Hoose et al., 2010), potentially affecting cloud formation and climate (Amato et al., 2007). Some microbial species, in fact, are able to freeze water at temperatures significantly warmer than those induced by nonbiological ice nucleators (-2 to -7 °C versus < -10 or -15 °C) (Morris et al., 2004). In the past, only a few attempts were made to directly measure the flux of bacteria from plant canopies (Lindemann et al., 1982; Lindemann and Upper, 1985; Lighthart and Shaffer, 1994; Crawford et al., 2014). Direct eddy covariance measurements of aerosol exchange in tropical forests, where PBAs represent a significant fraction of the airborne particulate matter (Graham et al., 2003), were also performed by Ahlm et al. (2010) and Whitehead et al. (2010), potentially giving a proxy for microbial emission in tropical ecosystems. The mass of PBAs that is actually released by different land use types under different conditions and, more importantly, the specific composition of such fluxes and their quantification remains so far mostly unresolved. As a consequence, numerical quantification of microbial emissions, as well as investigations of the effects of living biological particles on the atmosphere and the water cycle have been limited to highly idealized scenarios. Lighthart and Kirilenko (1998) attempted to simulate summertime diurnal emission dynamics, but in their work net upward fluxes were a function of time and solar-radiation-dependent microbial death only. Population dynamics in the phyllosphere and atmospheric turbulence were not accounted for. In their attempt to simulate global impacts of microbial particles on the water cycle, Hoose et al. (2010) and Sesartic et al. (2012) used fixed values of bacterial emission fluxes from different ecosystems, while Heald and Spracklen (2009) used mannitol as a proxy to evaluate fungal contributions to PBAs. Burrows et al. (2009a) modeled global emissions using data about airborne concentrations of microbes reported in the literature and derived fluxes from such proxies.

The aim of this paper is twofold: (i) to increase knowledge of microbial emissions by quantifying fluxes by means of a more complex micrometeorological method compared to earlier attempts and (ii) to propose a deterministic model to estimate both on-ground population dynamics and the associated atmospheric exchange processes.

The latter model was calibrated with microbial flux measurements made episodically over 3 years (between 2008 and 2010), while a second measurement campaign (2015) was used to validate its performance.

2 Materials and methods

2.1 Flux measurements

Microbial fluxes were measured during two field campaigns in a pasture in Montfavet, France (43.95° N, 4.88° E, 32 m a.s.l.). Measurements were made between 7 and 11 July 2015 and again between 26 September and 1 October 2015. The pasture was a typical Mediterranean grassland dominated by grasses in an area surrounded by similar land uses and with no significant orographic features. The vegetation status was different during the two campaigns: in July the grassland showed visible signs of water stress, but no more than 20 % of the leaves were chlorotic and dry. In September the grassland was instead well developed and mostly green. The mean height of the canopy was approximately 20 cm for both campaigns. The field was mainly covered with clover (*Trifolium* spp.) and ryegrass (*Lolium perenne*), was not intensively grazed, and was not actively managed during the measurement campaigns, with no mowing or irrigation.

Profiles of wind speed, air temperature and viable aerosols were made at two heights (≈ 70 and ≈ 250 cm), while a sonic anemometer (USA-1, Metek, Elmshorn, Germany; located at ≈ 300 cm) measured 3-D wind components and the sonic temperature at 20 Hz frequency. In September, an open-path infrared gas analyzer (Li-7500, LI-COR, Lincoln, Nebraska, USA) along with a differential infrared gas analyzer (Li-7000, LI-COR, Lincoln, Nebraska, USA) were added to the setup in order to concurrently measure the CO_2 and H_2O gas exchange using the eddy covariance and flux-gradient methods (Baldocchi et al., 1988). This setup (Fig. 1) allowed the assessment of the performance of the flux-gradient method of estimating water vapor fluxes vs. the respective fluxes directly measured by the eddy covariance method. Viable bioaerosols were sampled with Burkard jet samplers (Burkard Manufacturing Co. Ltd., Rickmansworth, UK). The samplers operated at a flow rate of 500 L min^{-1} and particles were collected on petri dishes containing 10 % tryptic soja agar (1.7 g of tryptone, 0.3 g of peptone soja, 0.25 g of glucose, 0.5 g of NaCl, 0.25 g of K_2HPO_4, 15 g agar L^{-1}). After sampling, the dishes were incubated at 25 °C and microbial colonies were counted after 24 h of incubation and for up to 3 days. Such a medium was nonselective, allowing the growth of both bacteria and fungi.

Sampling with each Petri dish lasted for 14 min and for every day a handling blank was incubated alongside the sampled plates.

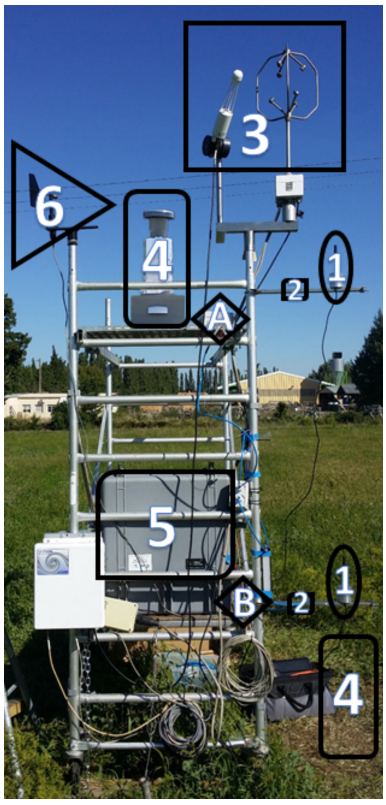

Figure 1. Schematic representation of the sampling station: each piece of equipment is represented by a number (in bold face) and the position of the equipment; all values in this caption are expressed in centimeters above ground level. Cup anemometers (1; 80 and 210), thermocouples (2; 80 and 210), sonic anemometer and Li-7500 open-path gas analyzer (3; 300), Burkard air samplers (4; 75 and 255; the bottom one is not in place in the figure, but the rectangle indicates its approximate position), Li-7000 differential gas analyzer (5; with inlets at 55 A and 200 B), and wind vane (6; 250).

The design of the virtual impactor followed good design practices with a direct alignment of the nozzle and the collection probe (i.e., the still air chamber), and diameter of the collection probe (0.08 m) was at least 40 % larger than the nozzle diameter (Marple and Olson, 2011). Data from literature indicate a sampling efficiency ranging from 80 to 100 % for mildew spores (Schwarzbach, 1979). Given the Burkard sampler's high flow rate, sampling happens at a super-iso-mean-velocity compared with external wind speed. The sampling efficiency is therefore expected to decrease for larger particles proportionally with the ratio between external wind speed and the Burkard's sampling speed (Brockmann, 2011).

A series of 10 min samplings with the Burkard samplers kept at the same height were performed to evaluate the minimum resolvable gradient (MRG) following Eq. (1) below (Edwards et al., 2005; Fritsche et al., 2008). ANOVA was used to verify the absence of significant difference in the number of colonies counted between the two samplers.

$$\mathrm{MRG} = (|(\overline{A-B})|) + \sigma(A-B), \quad (1)$$

where A indicates the sequence of the number of colonies in the top sampler, B indicates the sequence of the number of colonies in the bottom sampler and σ is the standard deviation of the respective differences.

The flux-gradient method was used to estimate microbial fluxes from concentrations measured with the Burkard samplers. This methodology has been widely used to measure atmospheric fluxes of different scalars such as hydrogen (Meredith et al., 2014), nitrates and nitrogen compounds (Beine et al., 2003; Griffith and Galle, 2000; Taylor et al., 1999), mercury (Edwards et al., 2005; Fritsche et al., 2008; Lindberg et al., 1995), and particulate matter (Bonifacio et al., 2013; Kjelgaard et al., 2004; Park et al., 2011; Sow et al., 2009). The method follows the Monin–Obukhov similarity theory (Monin and Obukhov, 1954) and therefore assumes that in the atmospheric surface layer the flux of a certain scalar is a function of the gradient of the scalar measured at different heights, the heights themselves (z_i), and a transport velocity that is dependent on atmospheric turbulence and stability (a more detailed description of the methodology is provided in the Supplement).

The measurement setup was chosen to avoid sampling in the roughness sub-layer, where the scaling principles do not hold and a conservative roughness length ($z0 = 0.15$ m) was chosen (Businger, 1986). This length was adequate to obtain a $z/z0 > 1$ (Businger, 1986) at both the low and high sampling heights, thus offsetting the presence of upwind obstacles that were within the range of the required horizontal surface uniformity (≈ 25 times z meters; Irvine et al., 1997). In keeping with the cited literature, fluxes are reported from the perspective of the atmosphere as positive when upward (i.e., emissions) and negative when downward (i.e., sinks).

A similar setup was employed between 2008 and 2010 to measure PBAs in an area very close by (43.91° N, 4.87° E and roughly 30 m a.s.l.). The Burkard samplers were deployed in a gradient configuration (at 50 and 250 cm above ground) along with a nearby sonic anemometer stationed at roughly 230 cm above the ground. No trace gas measurements were made during this period. The experimental field for these previous campaigns was covered with herbaceous species with similar habitus such as cocksfoot (*Dactylis glomerata*), ryegrass, tall fescue (*Festuca arundinacea*) and alfalfa (*Medicago sativa*). In the 2008–2010 campaigns a different methodology was used to assess the sampling differences between the two Burkard samplers. The two samplers were put together and a serial dilution of *P. syringae* was aerosolized. Three replicate samples were taken per each dilution (10^2, 10^3 and 10^4 live bacteria per mL) and no statistical differences were detected in the colony-forming units (CFUs) sampled by the Burkard samplers, with the single exception of one replicate at the 10^3 dilution. All the tests were

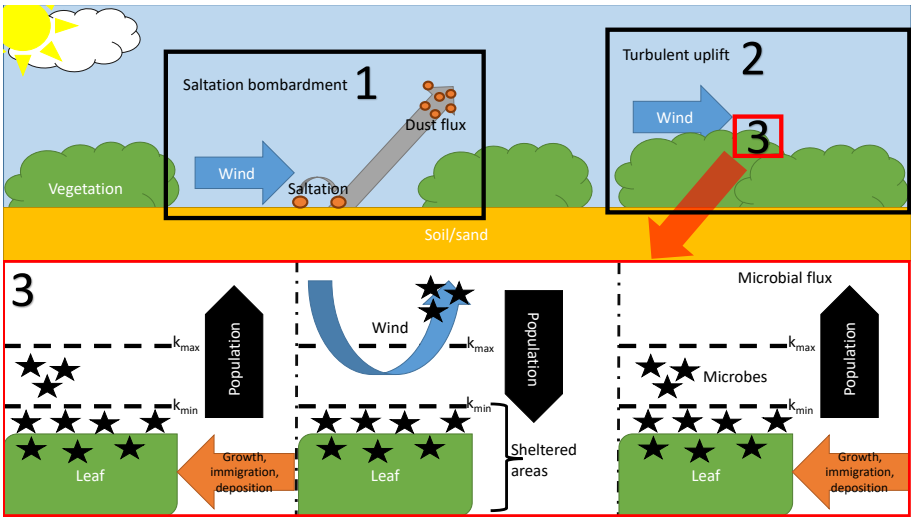

Figure 2. Schematics of the differences between Aeolian dust flux and microbial flux on which the PLAnET model is founded. Box 1 (top left) shows the typical dust saltation mechanism. The action of wind (blue arrow) on soil makes dust particles (orange dots) "jump" for short distances, ejecting smaller dust particles in the atmosphere. Turbulent uplift is shown in box 2 (upper right) where wind acts on the phyllosphere. What happens in the small red box 3 is indicated in more detail in the lower part of the figure (as indicated by the red arrow). The phyllosphere harbors a given number of microbial particles (black stars) up to a maximum (carrying capacity, k_{max} in the figure). Wind can remove a certain fraction of "available" microorganisms up to the limit of a sheltered fraction of the population (k_{min} in the figure). While the action of wind decreases the number of particles on the leaf, the population keeps experiencing phenomena such as growth, immigration from other leaves and deposition of airborne particles, all contributing to an increase in population. The balance between population dynamics and uplift is what contributes to the net flux simulated by the PLAnET model.

conducted with an open petri dish used to verify the deposition of the aerosolized spray.

2.2 The Plant–Atmosphere Epiphytic Transport (PLAnET) model

The model estimates microbial fluxes from the phyllosphere via a set of meteorological variables (air temperature, friction velocity and wind speed), the leaf area index (LAI) and atmospheric pressure. The model assumes that soil is an insignificant source of microorganisms for the atmosphere compared to the plant canopy. Other studies have considered that plant materials are the largest source of fungal spores in the atmosphere (Burge, 2002) and have shown that bacterial fluxes are higher over plants, except in cases of relatively rare events such as dust storms (Lindemann et al., 1982; Lindemann and Upper, 1985). This is in agreement with the finding that higher wind speeds are necessary to free a particle from soil rather than from the plant canopy (Jones and Harrison, 2004).

The model is based on three fundamental modules:

1. Source. Microbial population dynamics are driven by temperature, humidity, immigration–emigration phenomena, and competition (both between the microbial species and between plants and pathogens), and these factors change throughout space and time. To reduce the complexity of such interactions, the PLAnET model limits the representation of the microbial source to its main driver as a temperature-dependent growth function.

2. Removal. This is an energy-driven process. Wind shear and buoyancy act on the microbial population making a fraction of it airborne.

3. Deposition. Microbial deposition is computed as the product of a settling velocity and an airborne concentration estimated on LAI. The settling velocity itself is a linear combination of gravitational settling (computed following Kulkarni et al., 2011) and impaction–interception (computed following Slinn, 1982).

The gross upward flux of microbes into the atmosphere was simulated following a logistic equation (Eq. 2), assuming the existence of a threshold friction velocity (Aylor et al., 1981; Geagea et al., 1997). When simulating dust emissions it is generally assumed that there is a linear (Raupach and Lu, 2004) or exponential (Gillette and Passi, 1988) relationship between upward dust flux and friction velocity (u_*), due to the existence of saltation bombardment (Raupach and Lu, 2004; Dupont et al., 2013). Phyllosphere microbial populations are far from comparable to the soil surface on which such bombardment occurs and, therefore, a different mechanism has been chosen in the present context. It is assumed that no saltation mechanisms can intervene in amplifying particle removal and thus the upward flux will saturate at a certain u_*. The idea for this representation of the upward flux

is summed up in Fig. 2.

$$F_e = \left\{\left[m_1 \exp\left(-m_2 \exp^{(-m_3 u_*)}\right)\right]\right\} \frac{N}{k_{\max}} \quad (2)$$

In Eq. (2) F_e is the gross upward flux (in CFU $m^{-2}\,s^{-1}$); m_1, m_2, and m_3 are, respectively, $30\,\mathrm{CFU\,m^{-2}\,s^{-1}}$, $256.26\,\mathrm{CFU\,m^{-2}\,s^{-1}}$ and $19\,\mathrm{CFU\,m^{-2}\,s^{-1}}$ and were derived though a curve fitting to the Lighthart and Shaffer (1994) flux data with FOOTPRINT92 u_* data (Lighthart and Shaffer, 1994) and the model calibration procedure; N is the phyllosphere population in the model (in $\mathrm{CFU\,m^{-2}}$), and $k_{\max}$ is the maximum allowed microbial population (carrying capacity in $\mathrm{CFU\,m^{-2}}$).

If only wind speed, instead of wind speed and friction velocity, is provided as an input, the model calculates u_* using Eq. (3):

$$u_* = \frac{k\,u}{\ln \frac{z}{z0}}. \quad (3)$$

In Eq. (3) $k = 0.4$ and is the von Kármán constant, u is the wind speed (in $\mathrm{m\,s^{-1}}$), z is the sampling height in meters and $z0$ is the roughness length ($= 0.15$ m).

The gross downward flux (i.e., deposition) is modeled following Eq. (4):

$$F_\mathrm{d} = \left(V_\mathrm{g} + V_\mathrm{i}\right) C_\mathrm{a}. \quad (4)$$

F_d is the deposition flux ($\mathrm{CFU\,m^{-2}\,s^{-1}}$), V_g the gravitational settling velocity ($\mathrm{m\,s^{-1}}$), V_i ($\mathrm{m\,s^{-1}}$) the settling velocity due to impaction–interception from roughness elements and C_a the airborne concentrations of microorganisms ($\mathrm{CFU\,m^{-3}}$).

V_g is calculated following (Kulkarni et al., 2011) (Eq. 5):

$$V_\mathrm{g} = \frac{g \rho_\mathrm{p} d^2 C_c}{18\eta}, \quad (5)$$

where g is the gravitational acceleration ($9.81\,\mathrm{m\,s^{-2}}$), ρ_p is the particle density ($1100\,\mathrm{kg\,m^{-3}}$, Cox and Wathes, 1995), d is the particle diameter (3.3×10^{-6} m, Raisi et al. (2013) and Schlesinger et al., 2006), C_c is the Cunningham slip correction factor, and η is the air viscosity (1.83×10^{-5} Pa s, Kulkarni et al., 2011).

The term V_i represents the effect of interception–impaction on particle deposition and it has been computed following Slinn (1982):

$$V_i = C_d u_\mathrm{r} \left(1 + \frac{u_\mathrm{h}}{u_\mathrm{r}} \frac{1-\epsilon}{\epsilon + \sqrt{\epsilon}\tanh\gamma\sqrt{\epsilon}}\right)^{-1}, \quad (6)$$

where C_d is the ratio between u_*^2 and u_r^2, u_r represents wind speed measured at a reference height (in $\mathrm{m\,s^{-1}}$), u_h is wind speed measured at canopy height (in $\mathrm{m\,s^{-1}}$) and ϵ is the particle–canopy element collection efficiency (adimensional). The latter has been computed following Slinn (1982), but without accounting for diffusional effects (E_B in the cited paper) since they are not significant for particles > 1 µm (Wiman and Ågren, 1985). Equation (6) has the form of a velocity (being essentially a scaling factor for wind speed) and, when combined with V_g (see Eqs. 4 and 5), determines the actual particle deposition velocity. To solve Eq. (6), two wind speeds are needed (measured at canopy height and at a reference height above canopy), the ratio of which can be expressed as

$$\frac{u_\mathrm{h}}{u_\mathrm{r}} = \frac{u_*}{k u_\mathrm{r}} \ln \frac{l}{z_0}, \quad (7)$$

where l is a characteristic eddy size in the canopy (expressed in meters), which, in the present simplified implementation of the Slinn model, has been considered equal to canopy height (h; Slinn, 1982). Following Slinn's work, the parameter γ has been assumed to equal $\mathrm{h}^{1/2}$, while the other constants were set as $c_v/c_d = 1/3$, $\breve{\mathrm{A}} = 10\,\mu$m, $\hat{\mathrm{A}} = 1$ mm, $f = 1\,\%$, $b = 2$ and $c_\mathrm{Stk} = 1$.

The term C_a has been calculated as a characteristic seasonal airborne concentration for a Mediterranean grassland via a linear relationship between LAI values and average concentrations between the top and bottom sampler during the 2008–2010 campaign following Eq. (8):

$$C_\mathrm{a} = p_1 \mathrm{LAI} + p2. \quad (8)$$

In Eq. (8) $p1 = 26.99$ CFU $\mathrm{m^{-3}}$ and $p2 = 115.9\,\mathrm{CFU\,m^{-3}}$. LAI values used in this study were obtained from MODIS data (Myneni et al., 2015). Four 500 m pixels were averaged in space and interpolated in time to the half-hourly time series from the 4-day LAI time step of the satellite data. The average between-pixel standard deviation was quite consistent, varying slightly between ±0.32 and ±0.35 across all the simulated years.

The actual net PBA flux at a given time (F_n, $\mathrm{CFU\,m^{-2}\,s^{-1}}$) is computed following Eq. (9):

$$F_n = F_e - F_d. \quad (9)$$

The phyllosphere microbial population (N; see Eq. 2) is modeled following Eq. (10):

$$N = rN - (F_n \xi). \quad (10)$$

The growth rate r of Eq. (10) is modeled as a temperature-driven process in Eq. (11) (Yan and Hunt, 1999; Yin et al., 1995; Magarey et al., 2005):

$$r = \begin{cases} 0 \text{ if } T < T_\mathrm{MiN} \\ \left(\frac{T_\mathrm{MAX} - T}{T_\mathrm{MAX} - T_\mathrm{OPT}}\right)\left(\frac{T - T_\mathrm{MIN}}{T_\mathrm{OPT} - T_\mathrm{MIN}}\right)^{\left(\frac{T_\mathrm{OPT} - T_\mathrm{MIN}}{T_\mathrm{MAX} - T_\mathrm{OPT}}\right)} \\ c \text{ if } T_\mathrm{MIN} \le T \le T_\mathrm{MAX} \\ 0 \text{ if } T > T_\mathrm{MAX}. \end{cases} \quad (11)$$

In Eq. (9) T_MIN, T_MAX and T_OPT are, respectively, the minimum, maximum and optimal growth temperatures (in °C).

Table 1. Estimates for model parameters. The parameters tagged with an asterisk (*) are those that entered the calibration as unknowns from the initial guess, while the other parameters were fixed.

Parameter	Range boundaries	References for ranges	Units
T_{MIN}*	5–15	Standard mesophilic range	°C
T^*_{MAX}	30–45	Standard mesophilic range	°C
T_{OPT}	T_{MIN}–T_{MAX}	Standard mesophilic range	°C
c^*	0.12	Inserted by the authors	None
k^*_{min}	4.7×10^4–4.7×10^5	Hirano and Upper (1986); Wilson and Lindow (1994)	CFU m^{-2}
k^*_{max}	4.7×10^5-4.7×10^8	k_{min} and Hirano and Upper (1986)	CFU m^{-2}
m^*_1	22.3–35	Derived by the authors from Lighthart and Shaffer (1994)	CFU m^{-2} s^{-1}
m^*_2	250–260	Derived by the authors from Lighthart and Shaffer (1994)	CFU m^{-2} s^{-1}
m^*_3	17–23.3	Derived by the authors from Lighthart and Shaffer (1994)	None
ξ	1800	Eq. (10)	Seconds
p_1	26.99	Derived by the authors	CFU m^{-3}
p_2	115.9	Derived by the authors	CFU m^{-3}

c is a calibration constant accounting for the unknown doubling time of the microbes in the phyllosphere. For the purpose of Eq. (10) the net flux is multiplied by the model time step ($\xi = 1800$ s) making the units of the second right-hand term coherent with the units of the first right-hand term (rN, CFU m^{-2}).

The model also includes two thresholds: a minimum (k_{min}, a number of microorganisms sheltered by wind action following the concept of Waggoner, 1973) and a maximum population size (k_{max} or carrying capacity, which is the maximum population that an ecosystem can sustain indefinitely; Verhulst, 1838). When the population falls below k_{min} no removal can happen and if the population overshoots k_{max}, no growth can happen. Since the model is focused on phyllosphere dynamics, k_{max} is appropriately scaled with LAI in order to represent plant senescence and therefore the reduced availability of space and resources. The model starts from an estimate of the initial population (N_0), representing the "boundary condition" for the modeled processes at the start of the simulation and proceeds with half-hourly time steps until the end of the simulation period.

2.3 Model calibration and sensitivity analysis

The model was run between 1 January 2008 and the 31 December 2010, assuming that the microbial population in the phyllosphere at the beginning of the period was equal to k_{min} due to low LAI and temperature. The error metric to evaluate model performance is described by Eq. (12):

$$\varepsilon = |(1 - |s|)| + |o| + |(1 - \left|r^2\right|)|. \quad (12)$$

In Eq. (12), ε represents the error metric, s the slope of the linear relationship between measured and modeled net fluxes, o the offset of this relationship and r^2 the correlation coefficient. The function receiving the model parameters as input and returning ε as an output was passed to MATLAB's fmincon interior-point algorithm (Byrd et al., 1999, 2000; Waltz et al., 2006) as the objective function for minimization. The algorithm was run iteratively through MATLAB's GlobalSearch function in order to avoid finding a set of parameters satisfying only a local minimum. To avoid mathematically sound, but nonrealistic solutions, GlobalSearch was looking for minima only within a bounded parameter space. The upper and lower bounds of the parameter space are shown in Table 1. The percentage of leaf area exposed to turbulence was arbitrarily estimated to correspond to 5 % of the average leaf area density of the grassland that was set at 94 g m^{-2} (Sims and Singh, 1978). The latter assumption was needed to scale the measurements of Hirano and Upper (1986) and Wilson and Lindow (1994) in CFU per gram to the units needed by the model (CFU m^{-2}).

The calibrated model was then run on the data collected in 2015 in order to assess its performance on a dataset not used for training. Optimal temperature was not entered as a calibration parameter but was assumed to be halfway between the T_{MIN} and T_{MAX} chosen by the optimization algorithm.

Sensitivity of the model was analyzed by computing new values of ε by varying each parameter by plus and minus 10 %. For each parameter, a mean ε was computed by averaging the two errors resulting from the up and down modifications. Finally, a sensitivity metric was obtained by simply subtracting the ε obtained by the optimization procedure from the average error of each parameter.

3 Results

3.1 Field measurements

During the 2015 campaigns, temperature ranged between 13.4 and 34.1 °C (mean 25.2 ± 6 °C, right y axis Fig. 3a). Wind speed fluctuated between 0.2 and 5.3 m s^{-1} (mean

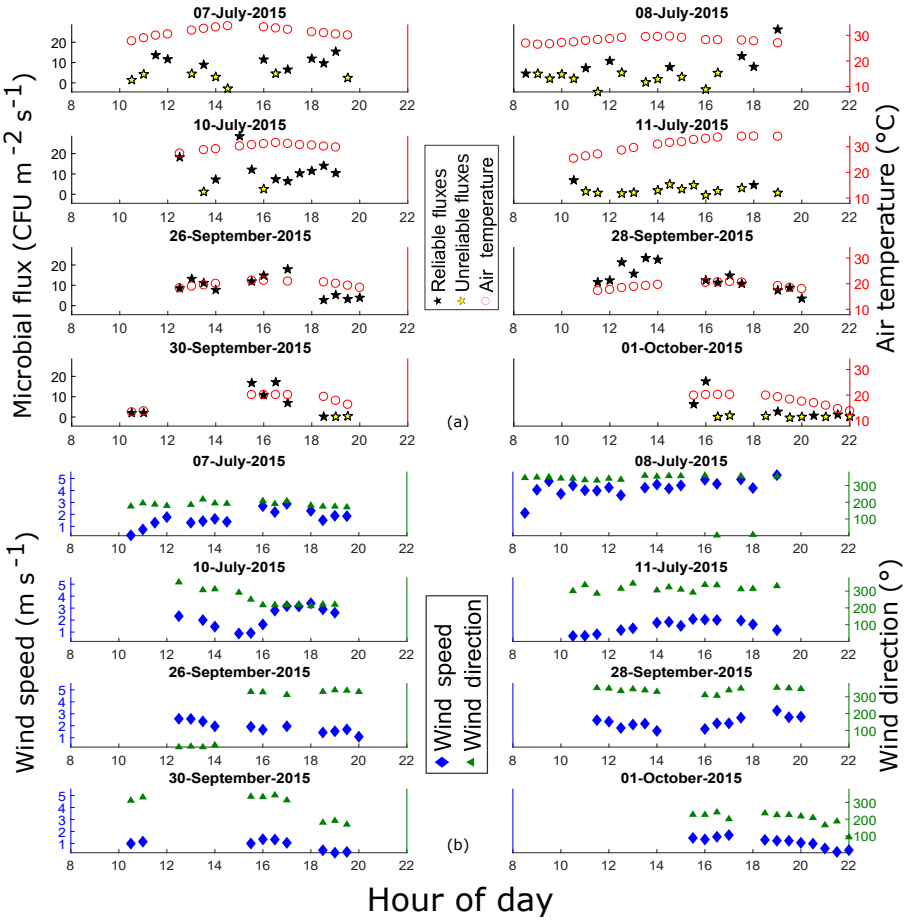

Figure 3. Dynamics of observed microbial fluxes, air temperature, wind speed and wind direction in the 2015 field campaigns. Panel **(a)** shows the time series of air temperature and microbial fluxes for July and September–October 2015. Unreliable fluxes are those below the MRG. Panel **(b)** shows the time series of wind speed and wind direction for the same periods.

Table 2. Results of the optimization procedure and the sensitivity analysis. The first row reports the value chosen by the optimization for the parameters in the column headers, while the second row reports the sensitivity value for each parameter.

	T_{MIN} (°C)	T_{MAX} (°C)	c	k_{min} (CFU m^{-2})	k_{max} (CFU m^{-2})	m_1	m_2	m_3
Value	12.96	30.16	0.13	5×10^4	4.82×10^6	30	256.26	19
Sensitivity	0.65	0.29	0.23	0.03	0.23	0.35	0.08	0.47

2.1 ± 1.2 m s^{-1}, left y axis Fig. 3b) with a general northerly wind direction (right y axis Fig. 3b). During the same campaign, fungal colonies dominated the microbial colonies growing on culture media, but bacterial-like colonies were also present. Measured microbial fluxes varied both between and within the days of the two field campaigns (July and September, left y axis Fig. 3a), with individual flux measurements being above the MRG in 60.6 % of all cases. Unreliable fluxes were unevenly distributed between July and September and included all negative fluxes (i.e., deposition, left y axis Fig. 3a). In 2015, the plant canopy was a net microbial emitter (left y axis Fig. 3a), with net fluxes ranging between 0.2 and 28.5 CFU m^{-2} s^{-1}. An overview of the relationship between counted CFUs, MRG and estimated fluxes is presented in Fig. 4. In September 2015, fluxes of water vapor directly measured using eddy covariance were compared with the ones resulting from the application of the flux-gradient method, yielding a high correlation between the two ($r^2 = 0.70$) and with minimal bias ($y = 1.05x - 0.08$; RMSE = 0.79) (Fig. 5), thus showing the absence of divergences between the two methods.

The measurements between 2008 and 2010 were made in different seasons, resulting in a wider range of temperatures spanning from 7.9 to 28.1 °C (mean 18.5 ± 4.8 °C,

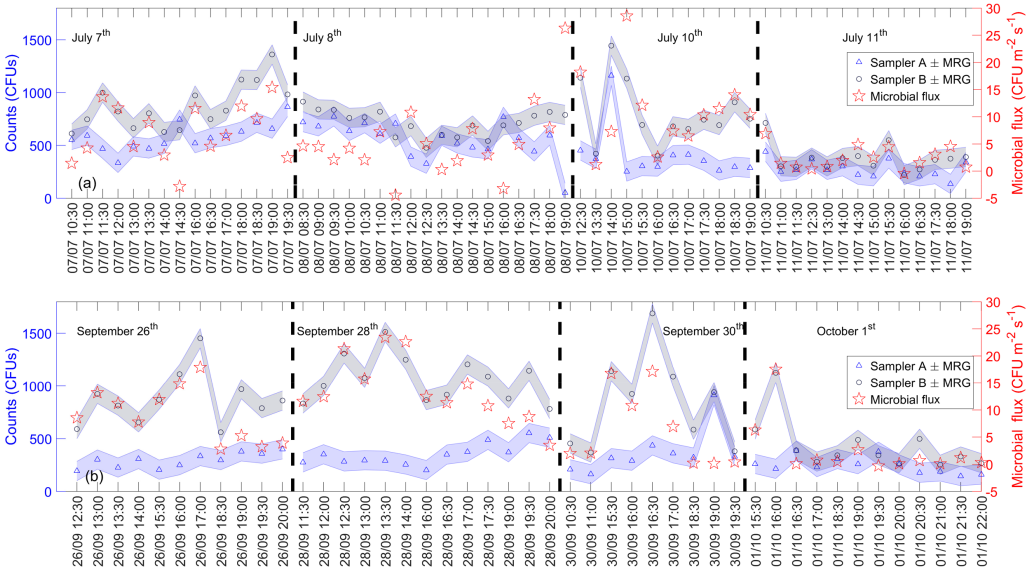

Figure 4. Details of the relationship between counted CFUs from the Burkard samplers and the estimated fluxes for the campaigns of July **(a)** and September **(b)** 2015.

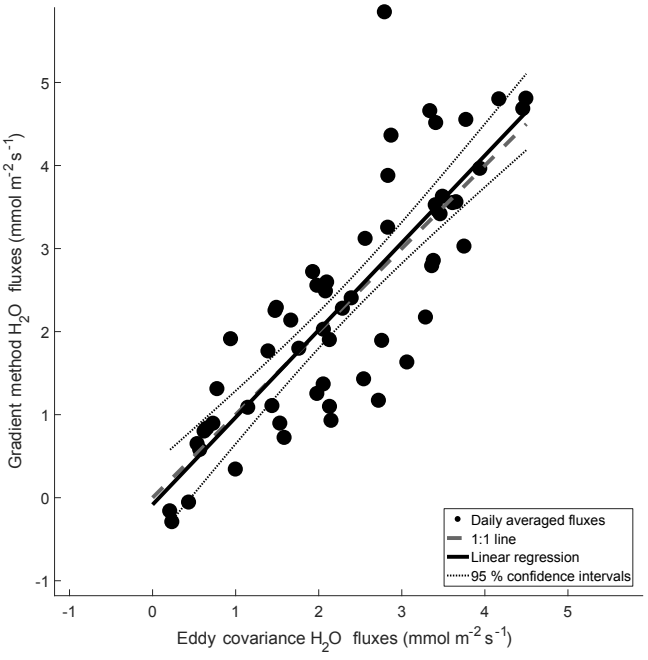

Figure 5. Water vapor fluxes measured via the eddy covariance method (x axis) vs. those derived from the flux-gradient method (y axis). The plotted linear regression has a slope of 1.05 and an offset of −0.08 and explains 70 % of the data variability.

right y axis Fig. 6a). Wind speed was consistent with the 2015 campaign, ranging from 0.4 to 5.8 m s^{-1} (mean 2.4 ± 1.4 m s^{-1}, left y axis Fig. 6b) with a mainly northerly wind direction (with the exception of 2009 for which no wind direction data were available, right y axis Fig. 6b). Microbial fluxes within these 3 years spanned a wider range of magnitude, varying between −5.2 and 57.1 CFU m^{-2} s^{-1} (left y axis Fig. 6a). The average flux between 2008 and 2010 was close to the 2015 average (8.3 CFU m^{-2} s^{-1} in 2008–2010 versus 10.6 CFU m^{-2} s^{-1} in 2015), while the standard deviation was higher (11.1 CFU m^{-2} s^{-1} in 2008–2010 versus 6.2 CFU m^{-2} s^{-1} in 2015). Few negative fluxes were registered in 2008–2010, which represented only 16.8 % of the total, confirming that the sampling site tended to be a net microbial emitter, rather than a sink.

3.2 Model calibration

The results of the optimization are resumed in Table 2 in which the chosen parameters are reported along with the respective sensitivity value.

All the chosen values fell within the imposed boundaries (see Table 1). The optimization procedure was able to find a meaningful optimum as it is deducible by looking at the sensitivity values reported in Table 2. Any variation in a parameter results in a worsening of the error metric (i.e., a positive sensitivity value), even if the model is not equally sensitive to all the parameters. More specifically, the minimum temperature regulating the growth curve of the microorganisms is the one with the highest impact on model performance, while the minimum population size ($k_{\min}$) seems to have the least impact. The latter result also suggests that the approximation made concerning the percent of leaf area exposed to turbulence (i.e., 5 %) is not critical.

Relationships between measured and modeled fluxes with an optimal set of parameters are reported in Fig. 7 for both the calibration set (2008–2010, Fig. 7a) and the validation campaigns (2015, Fig. 7b). The model is consistent between

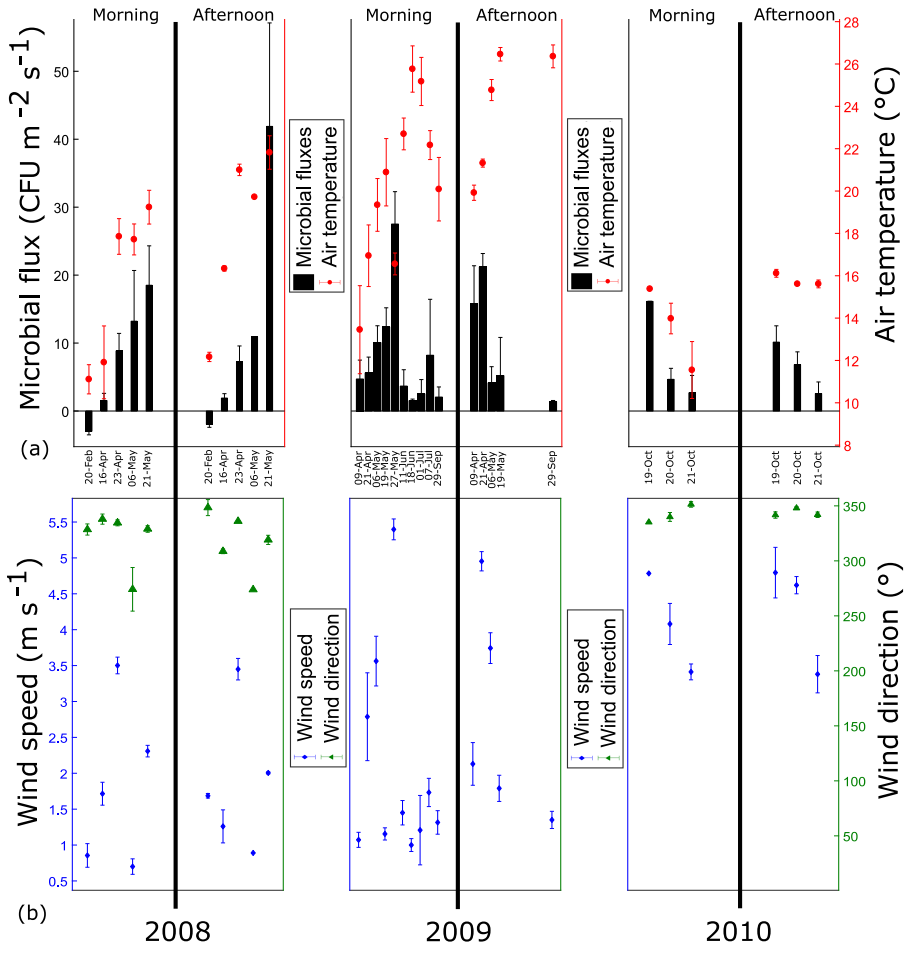

Figure 6. Temporal dynamics of observed microbial fluxes, air temperature, wind speed and wind direction in the 2008, 2009 and 2010 field campaigns. Panel **(a)** shows time series of air temperature and microbial fluxes for the campaigns held between 2008 and 2010. Panel **(b)** shows the time series of wind speed and wind direction for the same period. No wind direction data were available for the year 2009. For both **(a)** and **(b)** morning and afternoon averages are reported with the relative standard error in the error bars.

the two campaigns, explaining roughly 55–70 % of the variance (r^2 for 2008–2010 is 0.54 while r^2 for 2015 is 0.68) and it does it with a small offset (0.28 CFU m^{-2} s^{-1} in 2008–2010 and −3.75 CFU m^{-2} s^{-1} for 2015). The model still has a bias in the flux estimation: it tends to underestimate the fluxes during the calibration campaign (slope of the regression of 0.70) and overestimate them during the 2015 field campaigns (slope of the regression 1.31). The model has an RMSE of 5.82 CFU m^{-2} s^{-1} in 2008–2010, while it is 2.78 CFU m^{-2} s^{-1} for 2015.

Interestingly, while a clear dependence of the measured fluxes on atmospheric turbulence (u_*) was frequently observed, u_* was not always correlated with flux contrary to what might be expected. On some occasions, the measured microbial fluxes were much lower than predicted by Eq. (2), which directly scales the effect of turbulence on the microbial fluxes. This observation is consistent with the assumptions made in the PLAnET model, in which the actual microbial flux is indeed driven by turbulence but also constrained by the rate at which microorganisms multiply and by the size of the microbial population in the phyllosphere. This is represented graphically in Fig. 8a and b. When the population is close to the minimum population ($k_{\min}$), even very high turbulence (mean u_* for Fig. 8a is 0.49 m s^{-1}) will not elicit significant upward net fluxes. Conversely, when the microbial population is large (in Fig. 8b above 4.8×10^5 CFU m^{-2}), even low turbulence (mean u_* for Fig. 8b is 0.39 m s^{-1}) will generate significant upward net fluxes. Accordingly, the model was able to capture the variability in the number of CFUs that can be instantaneously transported into the atmosphere, thus predicting complex interactions between weather conditions, microbial population densities and the actual flux. This latter result suggests that for organic particles the simple knowledge of the transport field may not be enough: microbial populations have their own inherent dynamics (growth, death, immigration and em-

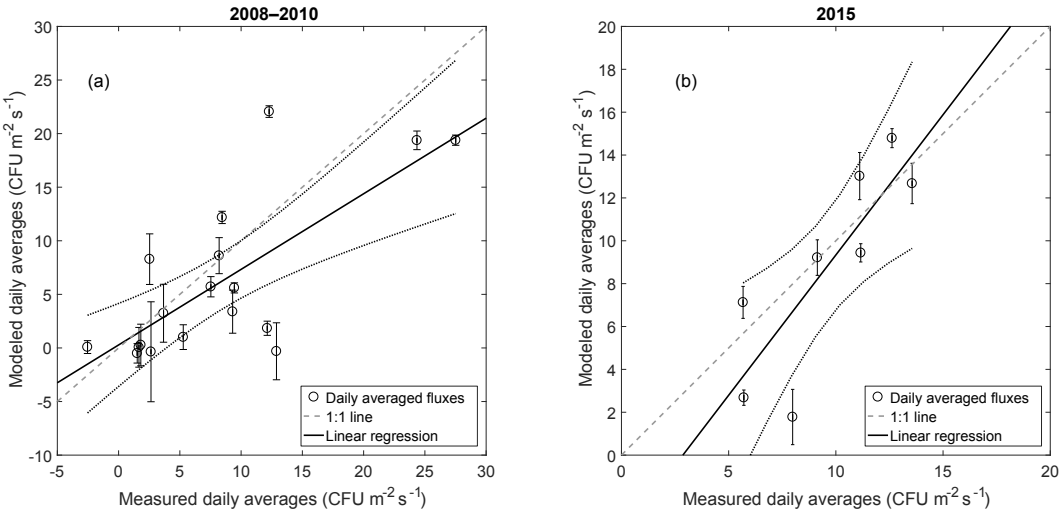

Figure 7. Relationship between measured and modeled daily averages of microbial flux. Figure 6a shows the regression between the daily averages from the 2008–2010 campaigns and the optimized model ($y = 0.70x + 0.28$; $r^2 = 0.54$) and Fig. 6b shows the one from the 2015 campaigns and the model ($y = 1.31x - 3.75$; $r^2 = 0.68$). The error bars are derived from the following equation: $\pm\sigma\left(\frac{m_i - o_i}{\overline{m_i, o_i}}\right)$, where σ is the standard deviation of the ratio between the difference between modeled and observed points ($m_i - o_i$) and the average of the same points ($\overline{m_i, o_i}$).

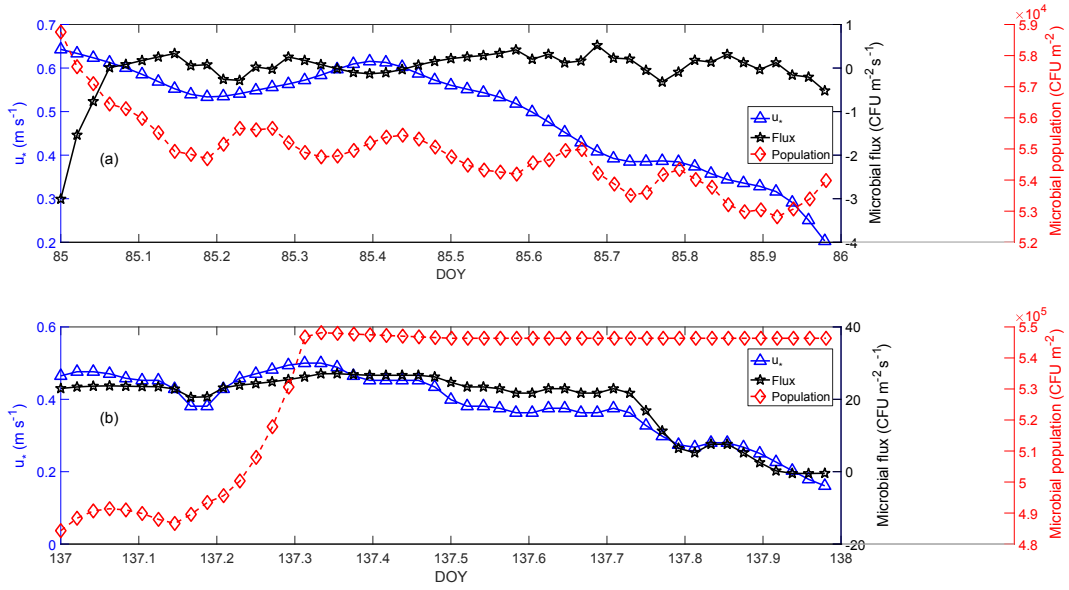

Figure 8. A high u_* / low flux event **(a)** and low u_* / high flux event **(b)** as simulated for the year 2015. The x axis indicates the fractional day of the year (DOY, Northern Hemisphere) for these two events, the left y axis shows the u_* values, the top far-right y axis shows the microbial net flux, and the bottom far-right y axis shows the phyllospheric population size.

igration) that influence the number of microbial cells available for transport. This phenomenon is clearly absent in the modeling of the dispersion of inorganic dust particles.

Simulated daily sums of PBA fluxes for the entire validation year are shown in Fig. 9. These are high from spring to early autumn, when temperatures are favorable for microbial and plant growth and sharply decrease during winter months in response to a decrease in temperature and LAI, an increase in the mean wind speed, and a decrease in the mean number of microorganisms populating the phyllosphere (Fig. 9). The model also predicts episodes in which the daily fluxes of microorganisms into the atmosphere are above and up to roughly twice that of the seasonal average. These events are often associated with persistent conditions of high wind and turbulence (Fig. 10a, b) and clear skies (Fig. 10c, d), which are typical of the synoptic weather conditions in southeast-

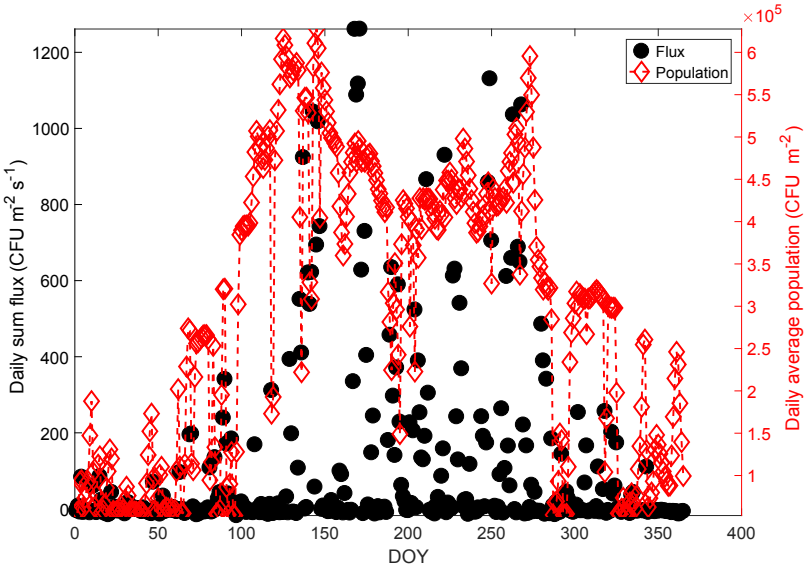

Figure 9. Time series of the daily sum of modeled microbial fluxes and daily averages of the surface microbial population for 2015. The labels on the *x* axis define the DOY starting from 1 January 2015 (DOY 1, Northern Hemisphere winter) to 31 December 2015 (DOY 365, Northern Hemisphere winter).

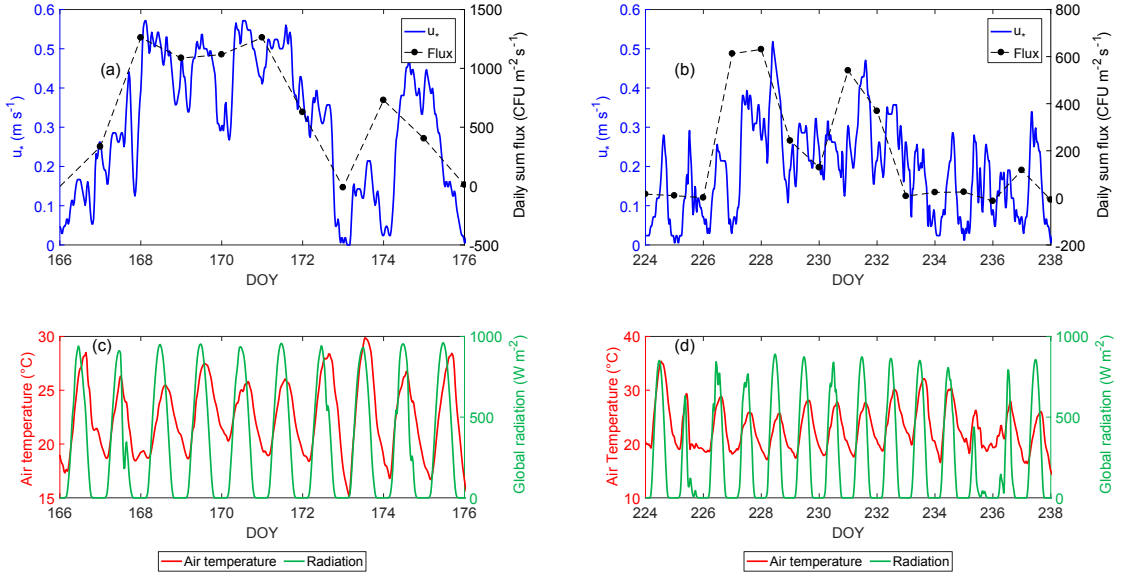

Figure 10. High wind events in 2015 in Montfavet, France. Plots **(a)** and **(b)** show friction velocity (left *y* axis) and the daily sum of flux (right *y* axis) for two high wind events (DOY 166–176 and 224–238 of 2015). Plots **(c)** and **(d)** show solar radiation (right *y* axis) and air temperature (left *y* axis) for the same two events.

ern France, when high pressure in the Bay of Biscay and a low around the Gulf of Genoa generate the wind that prevails from the north (called the "mistral"). Under these favorable conditions microbial growth in the phyllosphere balances the high removal rates caused by turbulence, so that the overall microbial population on leaves sustains high transport (Fig. 10c).

4 Discussion

The results and tools we present here offer a new approach for studying bioaerosols. Previous attempts to understand the distribution of PBAs in the atmosphere tended to simplify the surface–atmosphere transport both by deriving emissions from airborne concentrations (Burrows et al., 2009a) and by making ecosystem-wide assumptions about emissions (Bur-

rows et al., 2009a; Hoose et al., 2010; Sesartic et al., 2012). Airborne concentrations are, nevertheless, variable, being the combined results of both emissive and depositional processes as well as atmospheric transport (Wilkinson et al., 2012). For this reason, we conceived the PLAnET model to estimate fluxes directly, while accounting for the underlying emission–deposition processes. We sought to capture the dynamics underlying microbial emissions, thereby making the airborne concentrations a direct consequence without further assumptions. The model tries to generate fluxes from the interactions of the phyllosphere population dynamics and the local meteorological conditions instead of employing only a regression framework from measured data (such as in a previous attempt to simulate microbial fluxes; Lighthart and Kirilenko, 1998). While both gross upward and downward fluxes in the PLAnET model are resolved separately, this does not happen when employing a gradient method, and the presence of depositional effects could affect the observed gradient. Following Gillette et al. (1974, 1997), depositional effects for particles $< 10\,\mu m$ are significant only when the ratio between the deposition and friction velocity is greater than 0.1.The value of this ratio did not exceed the critical thresholds either in the 2008–2010 campaigns or in 2015. This guarantees the applicability of the gradient method for the observations at the Montfavet site made in sufficiently turbulent conditions. Depositional effects were also not relevant in Park et al. (2011) when applying the gradient method to PM_{10} fluxes. It has to be taken in account, though, that deposition depends on the particle diameter, and the choice of a fixed diameter for bioaerosols that was made here is a necessary simplification due to the impossibility of knowing the full size spectrum and its temporal variation. Seasonal variations in the size fraction containing most bioaerosols were in fact detected by Raisi et al. (2013).

The PLAnET deterministic framework follows the approach of Fall et al. (2016), which employed data from the literature on a specific pathogen, *Bremia lactucae,* to estimate its airborne concentrations. From Table 2 it is clear that the optimization procedure made a clear use of the imposed bounds in order to obtain feasible parameters. Not imposing feasible bounds would have posed a risk for the minimization to wander into physically unrealistic but mathematically sound parameter space (i.e., a set of parameters achieving a very small ε by combining, for example, nonrealistic growth temperatures). The optimal temperature chosen by the optimization algorithm for microbial growth, for example, is 21.6 °C. Considering that during summer days with higher vapor pressure deficit the leaf surface temperature can reach even a 5 °C difference from air temperature (Jackson et al., 1981; Wiegand and Namken, 1966), this would mean that the modeled optimal temperature is quite close to the incubation temperature used in the laboratory (25 °C). It is worth noting that, while a reasonable choice of growth temperature range was made for the overall microbial population, specific microorganisms may have different temperature optima. Future work can be done to fine-tune such a range of the species composition of the microbial source. The reliability of the optimization is backed up by the sensitivity analysis: any variation in the chosen parameters results in a worsening of the error statistic, as is clearly visible from Table 2.

Compared to the model by Fall et al. (2016), PLAnET falls short in terms of validation statistics. These differences can be explained by the different endpoints and scopes between the models. Since the PLAnET model aims to simulate an overall bioaerosol flux, instead of airborne concentrations of a single species as does the model by Fall et al. (2016), there are significantly higher uncertainties involved in the process. Nevertheless, if the confidence intervals (CIs) for the slopes in Fig. 7 are taken into account, it can be seen that in 2008–2010 and in 2015, the 95 % CIs include 1 and exclude 0 (the 95% CIs are 0.36–1.05 and 0.41–2.21, respectively). This suggests that the main weakness of the model would only be the number of observations. Longer campaigns conducted on different ecosystems would help in better assessing the relationship between modeled and measured data as well as the "portability" of the PLAnET model to different ecosystems.

While the results obtained are quite promising, there are still some caveats to consider. One of the first improvements that would benefit the PLAnET model would be validation on microbial fluxes that are not based solely on cultivated microorganisms. The ratio of culturable microorganisms to total microorganisms may range from 0.01 to 75 % and is generally below 10 % (see Burrows et al., 2009b, and references therein), meaning that PLAnET output needs scaling to be compared with the work, for example, of Burrows et al. (2009a), Sesartic et al. (2012) and Sesartic et al. (2013). A simple comparison can be made between PLAnET simulated fluxes and fluxes reported in Burrows et al. (2009a) using the scaling factor for the ratio of culturable to total bacteria for grasslands (302, Burrows et al., 2009b). An average total microorganism flux of $750.5 \pm 1976\,\text{cells}\,\text{m}^{-2}\,\text{s}^{-1}$ was obtained for PLAnET that, although associated with a high variability, is similar to the median value for grassland (roughly $1000\,\text{cells}\,\text{m}^{-2}\,\text{s}^{-1}$) reported in Burrows et al. (2009a). PLAnET can be used to predict microbial emissions and, when proper scaling factors are selected, it can potentially be used as a tool to link surface processes to the spatial and temporal dynamics of atmospheric processes since PBAs could represent an important component of the atmospheric aerosol load (at least on regional scales; Hummel et al., 2015). There are only a few quantitative, field-deployable sampling methods that target all microbial cells including non-culturable ones. One of the most reliable that can be adopted for analyzing samples coming from different kinds of collectors is epifluorescence staining, which is able to discriminate biological versus nonbiological particles in a sample independently from their culturability. Contrary to plate incubation, epifluorescence is also able to detect viable but non-culturable microbial cells, that is, organisms that are not dead but are not in the condition of growing

(see Oliver, 1993, and Burrows et al., 2009b, and references therein). The key issue with the method is the need for a minimum number of particles per sample ($10^4\,L^{-1}$; Gandolfi et al., 2013) and therefore an appropriate amount of sampled air. At rural sites, Bowers et al. (2011) were able to employ epifluorescence sampling at $30\,L\,min^{-1}$ for 1.5 h, while Harrison et al. (2005) worked with high-volumetric sampling at $1000\,L\,min^{-1}$ for 6 h at a time. Such timescales are not suitable for flux-gradient applications, for which fluctuations in concentrations must be resolvable on a timescale appropriate for the planetary boundary layer response time (≤ 1 h). This is why in the present work Burkard samplers were chosen: both for their high volumetric flow rate ($500\,L\,min^{-1}$) and for their virtual impactor nature that is favorable for preserving particle viability. Still, in future studies, epifluorescence sampling performed on "relatively long" time intervals (e.g., 1.5 h or more) could be used alongside more frequent (e.g., 15 min) cultivable samplings to scale cultivable to total microorganisms, assuming that the culturability does not change in the longer time span. Ultraviolet-induced laser fluorescence (UV-LIF) is a very recent methodology that measures PBA concentration from fluorescence emission and particle characteristics, using statistical methods such as hierarchical agglomerative cluster analysis to distinguish between different types of PBAs (Crawford et al., 2015). UV-LIF has already been used to measure atmospheric PBAs (Huffman et al., 2010; Gabey et al., 2010) and, given its relatively fast response time, it has the potential to be used in combination with micrometeorological methods to estimate microbial fluxes. A first attempt in this sense has been made in a pine forest by Crawford et al. (2014). This method is very promising since it works independently from microbial culturability, even if research is still ongoing on discriminating between different PBA classes and between PBAs and nonbiological fluorescent compounds contaminating the signal (Gabey et al., 2013; Pöhlker et al., 2012; Toprak and Schnaiter, 2013). Single-particle mass spectrometry (SPMS) is also a technique that can be used to detect PBAs by relying on the spectroscopic detection of specific compounds that are assumed as a proxy of bioaerosols (Zawadowicz et al., 2017). Similar to UV-LIF, this method does not rely on PBA culturability and suffers from interference of nonbiological particles with coincident spectral peaks (Zawadowicz et al., 2017). It is important to consider, though, that even if live and dead microorganisms would contribute to cloud-related processes due to their chemical and physical composition, the latter would not matter from an evolutionary perspective. Live cells have a chance of further transmitting their biological and chemical footprints to a wider microbial population. The latter would represent an ecological feedback increasing the population of live particles with characteristics that could favor survival and, eventually, physical interaction with atmospheric processes (i.e., increased expression of given proteins). While it is true that estimating fluxes of total biological particles is important from a biogeochemical point of view (Burrows et al., 2009a), measuring the viable fraction of fluxes would give information about the number of microorganisms that can potentially survive transport. The second critical improvement would be to validate and test the model on data from a larger number of different ecosystems, such as forests and agricultural crops.

Another caveat regards the parametrization of deposition. The simplified version of the model of Slinn (1982) implemented in PLAnET does not take into account the presence of potential negative gradients between atmosphere and canopy, which were not possible to investigate during the present sampling campaigns. This aspect needs further investigation for a better representation of particle deposition in such conditions.

The prognostic capability of the model has been investigated by running the model between 2001 and 2015. In the years when meteorological data from Montfavet were not available (2001–2006), we used the average of the closest four points from the Climate Forecast System Reanalysis hourly time series (Saha et al., 2010). Seasonally averaged net fluxes showed small interannual variation in winter when fluxes fluctuated around zero (-0.01 to $0.25\,CFU\,m^{-2}\,s^{-1}$) versus higher and more variable average fluxes in summer ranging from 3 to $8.3\,CFU\,m^{-2}\,s^{-1}$. The model was able to represent the interplay of the different meteorological variables: summer 2003 was characterized by one of the lowest average phyllosphere population sizes due to the exceptionally high temperatures registered during that year hindering microbial growth. In fact, in summer 2003 the average population size was $2.85 \times 10^5\,CFU\,m^{-2}$ versus a seasonal average of $3.86 \times 10^5\,CFU\,m^{-2}$ and an average temperature of 26 °C versus 23 °C. The lowest average summer population size was simulated, instead, in 2006 ($2.66 \times 10^5\,CFU\,m^{-2}$), when an unusually low LAI (0.8 versus 0.91 interannual seasonal average) influenced the maximum number of microorganisms that were able to grow along with a high average friction velocity increasing microbial removal (0.33 versus $0.25\,m\,s^{-1}$ interannual seasonal average). Still, there are some potentially unresolved meteorological forcings that the model does not take into account, such as rainfall. Huffman et al. (2013) and Prenni et al. (2013) provided convincing experimental evidence that bioaerosol and ice nucleator concentrations increased during and shortly after rainfall events. Rainfall, in fact, may boost PBA emissions. On the one hand, this may be due to the impact of raindrops that shake plants generating a detaching force (McCartney, 1991; Robertson and Alexander, 1994) and on the other hand it may be due to a boost in growth and a subsequent increase in the concentration of PBAs on the plant. For example, for *P. syringae* a 35-fold increase was seen after 48 h after a precipitation event (Hirano et al., 1996). This would increase the population of particles available for transport. This seems to contrast classical wet scavenging theory, in which falling hydrometeors deplete the atmosphere of suspended particles (Seinfeld and Pandis, 2012), and, therefore, act as a sink

for particulate matter (see, for example, Tai et al., 2010, or Ouyang et al., 2015). Due to this complex interaction between PBAs and rainfall, precipitation and humidity were not taken into account in this first version of the PLAnET model. In fact, if a very rainy month (September 2010 with an average of 0.13 mm of rain per hour) is compared against a non-rainy month (September 2007 with an average rainfall of $0.027\,\mathrm{mm\,h^{-1}}$), average net fluxes are very similar and actually greater in the less rainy month ($4.87\,\mathrm{CFU\,m^{-2}\,s^{-1}}$ in September 2007 versus $4.35\,\mathrm{CFU\,m^{-2}\,s^{-1}}$ in September 2010).

However, rainfall is not the only process that can influence net fluxes: intensive grazing, mowing and harvesting are also activities that can impact bioaerosol emission from a grassland. Such effects, however, are not straightforward and not completely known. Intensive grazing, for example, would damage the canopy, affecting LAI and the available population. Conversely, by damaging plants and releasing nutrients from plant tissue it could enhance microbial growth on leaves. Furthermore, animals themselves are potential bioaerosol sources (animal manure contains a large variety of microorganisms; Cotta et al., 2003). Harvesting would also contribute to the reduction of the source term (reducing LAI). However, along with many agricultural operations, harvesting can generate a higher amount of suspended particles (see, for example, Hiscox et al., 2008), potentially containing bioaerosols. All of these complex interactions can therefore generate both transient and lagged effects, which are still not taken into account by any model and should be investigated in the future.

5 Conclusions

With multiple campaigns this study investigated the behavior of a Mediterranean grassland from the point of view of microbial emissions. Across the campaigns, fluxes of microorganisms have been estimated through a sound micrometeorological method (flux-gradient methodology). The applicability of the method was assessed by comparing water vapor gradient fluxes with those measured directly by eddy covariance: the lack of significant divergence between the two suggests that the gradient methodology was applicable in the experimental conditions, even if it needs to be acknowledged that the good correspondence in terms of water vapor fluxes does not necessarily apply to bioaerosol flux measurements. Bacterial and fungal colonies, in fact, behave as a passive tracer in the absence of significant aerodynamic effects: such conditions were therefore tested during field campaigns using literature relationships between friction velocity and size of transported particles. The grassland showed a majority of emission fluxes, with a magnitude comparable to what was previously seen on a desert scrubland (Lighthart and Shaffer, 1994). The collected data were used to calibrate and validate a deterministic model (PLAnET) for estimating emissions of microorganisms from the surface. Even if there are still some open issues in the model (namely the relationship between flux, precipitation and the culturability of microorganisms), PLAnET provides previously unavailable insights into the dynamics of microbial fluxes and the underlying driving forces. Hopefully its evolution within the scientific community will be fostered not only by its ease of use (few easily accessible meteorological parameters are needed for its operation) but also by the robust framework for estimation of microbial fluxes (the model code can be freely downloaded at https://it.mathworks.com/matlabcentral/fileexchange/63257-planet-microbial-model). Its computational simplicity also makes it an attractive addition to larger-scale models aiming to simulate the dispersion of PBAs on regional or global scales (such as CALPUFF, Scire et al. (2000); WRF-CHEM, Grell et al. (2005); CHIMERE, Menut et al. (2013); ECHAM-HAM, Stier et al. (2005); or CAMx). The PLAnET model can in fact be an emission module receiving the same meteorological forcing of the dispersion model within which it is nested and generate time-varying emission rates at surface level. PBAs could be added as a chemical species with given characteristics, in addition to all the aerosols coming from biogenic and anthropogenic inventories. The larger-scale model would then be able to simulate the dispersion of the PBAs across the simulation domain, giving new insight in the potential of PBAs to impact precipitation, as well as exploring different scenarios about the potential pathways of transport of plant pathogens from the phyllosphere. In fact, given that some of the aforementioned models are able to simulate both gas-phase and aerosol chemistry, it would be possible to follow up the pioneering work of Burrows et al. (2009a) and Sesartic et al. (2013) on different spatiotemporal scales and investigate the changes in the outputs due to the insertion of a realistic PBA emission module.

Data availability. The model used in this text is available in the MathWorks repository as indicated in Sect. 5. All the other publicly available data employed (such as MODIS and GFS data) are correctly referenced in the text. As for the authors' microbial concentration and flux data, they are still undergoing processes for future publications and are therefore not eligible to be released publicly just yet.

The Supplement related to this article is available online at https://doi.org/10.5194/acp-17-14919-2017-supplement.

Competing interests. The authors declare that they have no conflict of interest.

Acknowledgements. Part of this work was funded thanks to the AirFors project (PIAPP-GA-2011-286079), part of the Seventh Framework European Programme. The authors wish to thank Alessandro Zaldei for his contribution to the preparation of the instrumentation for the 2015 campaign, as well as the technical and engineering staff from the INRA Unit of Plant Pathology (Jean-Marc Bastien, Joël Beraud, Jean-Francois Bourgeay, Frédéric Pascal and Michel Pascal) for their support during the field campaigns. A special thanks goes to André Chanzy (INRA) for his precious help on Montfavet meteorological data.

Edited by: Alex Huffman
Reviewed by: three anonymous referees

References

Ahern, H. E., Walsh, K. A., Hill, T. C. J., and Moffett, B. F.: Fluorescent pseudomonads isolated from Hebridean cloud and rain water produce biosurfactants but do not cause ice nucleation, Biogeosciences, 4, 115–124, https://doi.org/10.5194/bg-4-115-2007, 2007.

Ahlm, L., Krejci, R., Nilsson, E. D., Mårtensson, E. M., Vogt, M., and Artaxo, P.: Emission and dry deposition of accumulation mode particles in the Amazon Basin, Atmos. Chem. Phys., 10, 10237–10253, https://doi.org/10.5194/acp-10-10237-2010, 2010.

Amato, P., Parazols, M., Sancelme, M., Laj, P., Mailhot, G., and Delort, A.-M.: Microorganisms isolated from the water phase of tropospheric clouds at the Puy de Dôme: major groups and growth abilities at low temperatures, FEMS Microbiol. Ecol., 59, 242–254, https://doi.org/10.1111/j.1574-6941.2006.00199.x, 2007.

Aylor, D. E., McCartney, H. A., and Bainbridge, A.: Deposition of Particles Liberated in Gusts of Wind, J. Appl. Meteorol., 20, 1212–1221, https://doi.org/10.1175/1520-0450(1981)020<1212:tdosls>2.0.co;2, 1981.

Baldocchi, D. D., Hicks, B. B., and Meyers, T. P.: Measuring Biosphere-Atmosphere Exchanges of Biologically Related Gases with Micrometeorological Methods, Ecology, 69, 1331–1340, https://doi.org/10.2307/1941631, 1988.

Bauer, H., Giebl, H., Hitzenberger, R., Kasper-Giebl, A., Reischl, G., Zibuschka, F., and Puxbaum, H.: Airborne bacteria as cloud condensation nuclei, J. Geophys. Res.-Atmos., 108, 4658, https://doi.org/10.1029/2003JD003545, 2003.

Beine, H. J., Domine, F., Ianniello, A., Nardino, M., Allegrini, I., Teinila, K., and Hillamo, R.: Fluxes of nitrates between snow surfaces and the atmosphere in the European high Arctic, Atmos. Chem. Phys., 3, 335–346, https://doi.org/10.5194/acp-3-335-2003, 2003.

Bonifacio, H. F., Maghirang, R. G., Trabue, S. L., McConnell, L. L., Prueger, J. H., and Razote, E. B.: Particulate emissions from a beef cattle feedlot using the flux-gradient technique, J. Environ. Qual., 42, 1341–1352, https://doi.org/10.2134/jeq2013.04.0129, 2013.

Bowers, R. M., McLetchie, S., Knight, R., and Fierer, N.: Spatial variability in airborne bacterial communities across land-use types and their relationship to the bacterial communities of potential source environments, ISME J., 5, 601–612, https://doi.org/10.1038/ismej.2010.167, 2011.

Brockmann, J. E.: Aerosol Transport in Sampling Lines and Inlets, in: Aerosol Measurement, John Wiley & Sons, Inc., 68–105, 2011.

Brown, J. K. M. and Hovmøller, M. S.: Aerial Dispersal of Pathogens on the Global and Continental Scales and Its Impact on Plant Disease, Science, 297, 537–541, https://doi.org/10.1126/science.1072678, 2002.

Burge, H. A.: An update on pollen and fungal spore aerobiology, J. Allergy Clin. Immun., 110, 544–552, https://doi.org/10.1067/mai.2002.128674, 2002.

Burrows, S. M., Butler, T., Jockel, P., Tost, H., Kerkweg, A., Pöschl, U., and Lawrence, M. G.: Bacteria in the global atmosphere – Part 2: Modeling of emissions and transport between different ecosystems, Atmos. Chem. Phys., 9, 9281–9297, https://doi.org/10.5194/acp-9-9281-2009, 2009a.

Burrows, S. M., Elbert, W., Lawrence, M. G., and Pöschl, U.: Bacteria in the global atmosphere – Part 1: Review and synthesis of literature data for different ecosystems, Atmos. Chem. Phys., 9, 9263–9280, https://doi.org/10.5194/acp-9-9263-2009, 2009b.

Businger, J. A.: Evaluation of the Accuracy with Which Dry Deposition Can Be Measured with Current Micrometeorological Techniques, J. Clim Appl. Meteorol., 25, 1100–1124, https://doi.org/10.1175/1520-0450(1986)025<1100:EOTAWW>2.0.CO;2, 1986.

Byrd, R. H., Hribar, M. E., and Nocedal, J.: An Interior Point Algorithm for Large-Scale Nonlinear Programming, SIAM J. Opt., 9, 877–900, https://doi.org/10.1137/s1052623497325107, 1999.

Byrd, R. H., Gilbert, J. C., and Nocedal, J.: A trust region method based on interior point techniques for nonlinear programming, Mathematical Programming, 89, 149–185, https://doi.org/10.1007/pl00011391, 2000.

Cotta, M. A., Whitehead, T. R., and Zeltwanger, R. L.: Isolation, characterization and comparison of bacteria from swine faeces and manure storage pits, Environmental Microbiology, 5, 737–745, https://doi.org/10.1046/j.1467-2920.2003.00467.x, 2003.

Cox, C. S. and Wathes, C. M.: Bioaerosols Handbook Taylor & Francis, 656 pp., 1995.

Crawford, I., Robinson, N. H., Flynn, M. J., Foot, V. E., Gallagher, M. W., Huffman, J. A., Stanley, W. R., and Kaye, P. H.: Characterisation of bioaerosol emissions from a Colorado pine forest: results from the BEACHON-RoMBAS experiment, Atmos. Chem. Phys., 14, 8559–8578, https://doi.org/10.5194/acp-14-8559-2014, 2014.

Crawford, I., Ruske, S., Topping, D. O., and Gallagher, M. W.: Evaluation of hierarchical agglomerative cluster analysis methods for discrimination of primary biological aerosol, Atmos. Meas. Tech., 8, 4979–4991, https://doi.org/10.5194/amt-8-4979-2015, 2015.

Delort, A.-M., Vaïtilingom, M., Amato, P., Sancelme, M., Parazols, M., Mailhot, G., Laj, P., and Deguillaume, L.: A short overview of the microbial population in clouds: Potential roles in atmospheric chemistry and nucleation processes, Atmos. Res., 98, 249–260, https://doi.org/10.1016/j.atmosres.2010.07.004, 2010.

Dupont, S., Bergametti, G., Marticorena, B., and Simoëns, S.: Modeling saltation intermittency, J. Geophys. Res.-Atmos., 118, 7109–7128, https://doi.org/10.1002/jgrd.50528, 2013.

Edwards, G. C., Rasmussen, P. E., Schroeder, W. H., Wallace, D. M., Halfpenny-Mitchell, L., Dias, G. M., Kemp, R. J., and Ausma, S.: Development and evaluation of a sampling system

to determine gaseous Mercury fluxes using an aerodynamic micrometeorological gradient method, J. Geophys. Res.-Atmos., 110, D10306, https://doi.org/10.1029/2004JD005187, 2005.

Fall, M. L., Van der Heyden, H., and Carisse, O.: A Quantitative Dynamic Simulation of Bremia lactucae Airborne Conidia Concentration above a Lettuce Canopy, PLOS ONE, 11, e0144573, https://doi.org/10.1371/journal.pone.0144573, 2016.

Fritsche, J., Wohlfahrt, G., Ammann, C., Zeeman, M., Hammerle, A., Obrist, D., and Alewell, C.: Summertime elemental mercury exchange of temperate grasslands on an ecosystem-scale, Atmos. Chem. Phys., 8, 7709–7722, https://doi.org/10.5194/acp-8-7709-2008, 2008.

Fuzzi, S., Mandrioli, P., and Perfetto, A.: Fog droplets – an atmospheric source of secondary biological aerosol particles, Atmos. Environ., 31, 287–290, https://doi.org/10.1016/1352-2310(96)00160-4, 1997.

Gabey, A. M., Gallagher, M. W., Whitehead, J., Dorsey, J. R., Kaye, P. H., and Stanley, W. R.: Measurements and comparison of primary biological aerosol above and below a tropical forest canopy using a dual channel fluorescence spectrometer, Atmos. Chem. Phys., 10, 4453–4466, https://doi.org/10.5194/acp-10-4453-2010, 2010.

Gabey, A. M., Vaitilingom, M., Freney, E., Boulon, J., Sellegri, K., Gallagher, M. W., Crawford, I. P., Robinson, N. H., Stanley, W. R., and Kaye, P. H.: Observations of fluorescent and biological aerosol at a high-altitude site in central France, Atmos. Chem. Phys., 13, 7415–7428, https://doi.org/10.5194/acp-13-7415-2013, 2013.

Gandolfi, I., Bertolini, V., Ambrosini, R., Bestetti, G., and Franzetti, A.: Unravelling the bacterial diversity in the atmosphere, Appl. Microbiol. Biotechnol., 97, 4727–4736, https://doi.org/10.1007/s00253-013-4901-2, 2013.

Geagea, L., Huber, L., and Sache, I.: Removal of urediniospores of brown (Puccinia recondita f. sp. tritici) and yellow (P. striiformis) rusts of wheat from infected leaves submitted to a mechanical stress, Eur. J. Plant Pathol., 103, 785–793, 1997.

Gillette, D. A. and Passi, R.: Modeling dust emission caused by wind erosion, J. Geophys. Res.-Atmos., 93, 14233–14242, https://doi.org/10.1029/JD093iD11p14233, 1988.

Gillette, D. A., Blifford, I. H., and Fryrear, D. W.: The influence of wind velocity on the size distributions of aerosols generated by the wind erosion of soils, J. Geophys. Res., 79, 4068–4075, https://doi.org/10.1029/JC079i027p04068, 1974.

Gillette, D. A., Fryrear, D. W., Gill, T. E., Ley, T., Cahill, T. A., and Gearhart, E. A.: Relation of vertical flux of particles smaller than 10 µm to total aeolian horizontal mass flux at Owens Lake, J. Geophys. Res.-Atmos., 102, 26009–26015, https://doi.org/10.1029/97JD02252, 1997.

Graham, B., Guyon, P., Maenhaut, W., Taylor, P. E., Ebert, M., Matthias-Maser, S., Mayol-Bracero, O. L., Godoi, R. H. M., Artaxo, P., Meixner, F. X., Moura, M. A. L., Rocha, C. H. E. D. A., Grieken, R. V., Glovsky, M. M., Flagan, R. C., and Andreae, M. O.: Composition and diurnal variability of the natural Amazonian aerosol, J. Geophys. Res.-Atmos., 108, https://doi.org/10.1029/2003JD004049, 2003.

Grell, G. A., Peckham, S. E., Schmitz, R., McKeen, S. A., Frost, G., Skamarock, W. C., and Eder, B.: Fully coupled "online" chemistry within the WRF model, Atmos. Environ., 39, 6957–6975, 2005.

Griffin, D. W.: Atmospheric movement of microorganisms in clouds of desert dust and implications for human health, Clin. Microbiol. Rev., 20, 459–477, 2007.

Griffith, D. W. T. and Galle, B.: Flux measurements of NH_3, N_2O and CO_2 using dual beam FTIR spectroscopy and the flux–gradient technique, Atmos. Environ., 34, 1087–1098, https://doi.org/10.1016/S1352-2310(99)00368-4, 2000.

Harrison, R. M., Jones, A. M., Biggins, P. D., Pomeroy, N., Cox, C. S., Kidd, S. P., Hobman, J. L., Brown, N. L., and Beswick, A.: Climate factors influencing bacterial count in background air samples, Int. J. Biometeorol., 49, 167–178, https://doi.org/10.1007/s00484-004-0225-3, 2005.

Heald, C. L. and Spracklen, D. V.: Atmospheric budget of primary biological aerosol particles from fungal spores, Geophys. Res. Lett., 36, L09806, https://doi.org/10.1029/2009GL037493, 2009.

Hirano, S. and Upper, C.: Temporal, spatial, and genetic variability of leaf-associated bacterial populations, Microbiology of the phyllosphere, edited by: Fokkema, N. J. and van den Heuvel, J., 1986.

Hirano, S. S., Baker, L. S., and Upper, C. D.: Raindrop momentum triggers growth of leaf-associated populations of Pseudomonas syringae on field-grown snap bean plants, Appl. Environ. Microbiol., 62, 2560–2566, 1996.

Hiscox, A. L., Miller, D. R., Holmén, B. A., Yang, W., and Wang, J.: Near-Field Dust Exposure from Cotton Field Tilling and Harvesting All rights reserved. No part of this periodical may be reproduced or transmitted in any form or by any means, electronic or mechanical, including photocopying, recording, or any information storage and retrieval system, without permission in writing from the publisher, J. Environ. Qual., 37, 551–556, https://doi.org/10.2134/jeq2006.0408, 2008.

Hoose, C., Kristjánsson, J. E., and Burrows, S. M.: How important is biological ice nucleation in clouds on a global scale?, Environ. Res. Lett., 5, 024009, https://doi.org/10.1088/1748-9326/5/2/024009, 2010.

Huffman, J. A., Treutlein, B., and Pöschl, U.: Fluorescent biological aerosol particle concentrations and size distributions measured with an Ultraviolet Aerodynamic Particle Sizer (UV-APS) in Central Europe, Atmos. Chem. Phys., 10, 3215–3233, https://doi.org/10.5194/acp-10-3215-2010, 2010.

Huffman, J. A., Prenni, A. J., DeMott, P. J., Pöhlker, C., Mason, R. H., Robinson, N. H., Fröhlich-Nowoisky, J., Tobo, Y., Després, V. R., Garcia, E., Gochis, D. J., Harris, E., Müller-Germann, I., Ruzene, C., Schmer, B., Sinha, B., Day, D. A., Andreae, M. O., Jimenez, J. L., Gallagher, M., Kreidenweis, S. M., Bertram, A. K., and Pöschl, U.: High concentrations of biological aerosol particles and ice nuclei during and after rain, Atmos. Chem. Phys., 13, 6151–6164, https://doi.org/10.5194/acp-13-6151-2013, 2013.

Hummel, M., Hoose, C., Gallagher, M., Healy, D. A., Huffman, J. A., O'Connor, D., Pöschl, U., Pöhlker, C., Robinson, N. H., Schnaiter, M., Sodeau, J. R., Stengel, M., Toprak, E., and Vogel, H.: Regional-scale simulations of fungal spore aerosols using an emission parameterization adapted to local measurements of fluorescent biological aerosol particles, Atmos. Chem. Phys., 15, 6127–6146, https://doi.org/10.5194/acp-15-6127-2015, 2015.

Irvine, M., Gardiner, B., and Hill, M.: The evolution of turbulence across a forest edge, Bound.-Layer Meteorol., 84, 467–496, 1997.

Jackson, R. D., Idso, S. B., Reginato, R. J., and Pinter, P. J.: Canopy temperature as a crop water stress indicator, Water Resour. Res., 17, 1133–1138, https://doi.org/10.1029/WR017i004p01133, 1981.

Jones, A. M. and Harrison, R. M.: The effects of meteorological factors on atmospheric bioaerosol concentrations—a review, Sci. Total Environ., 326, 151–180, https://doi.org/10.1016/j.scitotenv.2003.11.021, 2004.

Kellogg, C. A. and Griffin, D. W.: Aerobiology and the global transport of desert dust, Trends Ecol. Evol., 21, 638–644, https://doi.org/10.1016/j.tree.2006.07.004, 2006.

Kjelgaard, J., Sharratt, B., Sundram, I., Lamb, B., Claiborn, C., Saxton, K., and Chandler, D.: PM_{10} emission from agricultural soils on the Columbia Plateau: comparison of dynamic and time-integrated field-scale measurements and entrainment mechanisms, Agr. Forest Meteorol., 125, 259–277, https://doi.org/10.1016/j.agrformet.2004.04.004, 2004.

Kulkarni, P., Baron, P. A., and Willeke, K.: Fundamentals of Single Particle Transport, in: Aerosol Measurement, John Wiley & Sons, Inc., 15–30, 2011.

Lighthart, B., Shaffer, B., Marthi, B., and Ganio, L.: Artificial wind-gust liberation of microbial bioaerosols previously deposited on plants, Aerobiologia, 9, 189–196, https://doi.org/10.1007/BF02066261, 1993.

Lighthart, B. and Shaffer, B. T.: Bacterial flux from chaparral into the atmosphere in midsummer at a high desert location, Atmos. Environ., 28, 1267–1274, https://doi.org/10.1016/1352-2310(94)90273-9, 1994.

Lighthart, B. and Kirilenko, A.: Simulation of summer-time diurnal bacterial dynamics in the atmospheric surface layer, Atmos. Environ., 32, 2491–2496, https://doi.org/10.1016/s1352-2310(98)00011-9, 1998.

Lindberg, S. E., Kim, K.-H., Meyers, T. P., and Owens, J. G.: Micrometeorological Gradient Approach for Quantifying Air/Surface Exchange of Mercury Vapor: Tests Over Contaminated Soils, Environ. Sci. Technol., 29, 126–135, https://doi.org/10.1021/es00001a016, 1995.

Lindemann, J. and Upper, C. D.: Aerial dispersal of epiphytic bacteria over bean-plants, Appl. Environ. Microbiol., 50, 1229–1232, 1985.

Lindemann, J., Constantinidou, H. A., Barchet, W. R., and Upper, C. D.: Plants as sources of airborne bacteria, including ice nucleation-active bacteria, Appl. Environ. Microbiol., 44, 1059–1063, 1982.

Magarey, R. D., Sutton, T. B., and Thayer, C. L.: A Simple Generic Infection Model for Foliar Fungal Plant Pathogens, Phytopathology, 95, 92–100, https://doi.org/10.1094/PHYTO-95-0092, 2005.

Marple, V. A. and Olson, B. A.: Sampling and Measurement Using Inertial, Gravitational, Centrifugal, and Thermal Techniques, in: Aerosol Measurement, John Wiley & Sons, Inc., 129–151, 2011.

McCartney, H.: Airborne dissemination of plant fungal pathogens, J. Appl. Bacteriol., 70, 39S–48S, 1991.

Menut, L., Bessagnet, B., Khvorostyanov, D., Beekmann, M., Blond, N., Colette, A., Coll, I., Curci, G., Foret, G., Hodzic, A., Mailler, S., Meleux, F., Monge, J. L., Pison, I., Siour, G., Turquety, S., Valari, M., Vautard, R., and Vivanco, M. G.: CHIMERE 2013: a model for regional atmospheric composition modelling, Geosci. Model Dev., 6, 981–1028, https://doi.org/10.5194/gmd-6-981-2013, 2013.

Meredith, L. K., Commane, R., Munger, J. W., Dunn, A., Tang, J., Wofsy, S. C., and Prinn, R. G.: Ecosystem fluxes of hydrogen: a comparison of flux-gradient methods, Atmos. Meas. Tech., 7, 2787–2805, https://doi.org/10.5194/amt-7-2787-2014, 2014.

Möhler, O., DeMott, P., Vali, G., and Levin, Z.: Microbiology and atmospheric processes: the role of biological particles in cloud physics, Biogeosciences, 4, 1059–1071, https://doi.org/10.5194/bg-4-1059-2007, 2007.

Monin, A. and Obukhov, A.: Basic laws of turbulent mixing in the surface layer of the atmosphere, Contr. Geophys. Inst. Acad. Sci. USSR, 151, 163–187, 1954.

Morris, C., Kinkel, L., Lindow, S., Hecht-Poinar, E., and Elliott, V.: Fifty years of phyllosphere microbiology: significant contributions to research in related fields, Phyl. Microbiol., 365–375, 2002.

Morris, C., Georgakopoulos, D., and Sands, D.: Ice nucleation active bacteria and their potential role in precipitation, J. Phys., 87–103, 2004.

Oliver, J. D.: Formation of Viable but Nonculturable Cells, in: Starvation in Bacteria, edited by: Kjelleberg, S., Springer US, Boston, MA, 239–272, 1993.

Ouyang, W., Guo, B., Cai, G., Li, Q., Han, S., Liu, B., and Liu, X.: The washing effect of precipitation on particulate matter and the pollution dynamics of rainwater in downtown Beijing, Sci. Total Environ., 505, 306–314, https://doi.org/10.1016/j.scitotenv.2014.09.062, 2015.

Park, M.-S., Park, S.-U., and Chun, Y.: Improved parameterization of dust emission (PM_{10}) fluxes by the gradient method using the Naiman tower data at the Horqin desert in China, Sci. Total Environ., 412–413, 265–277, https://doi.org/10.1016/j.scitotenv.2011.09.068, 2011.

Peter, H., Hörtnagl, P., Reche, I., and Sommaruga, R.: Bacterial diversity and composition during rain events with and without Saharan dust influence reaching a high mountain lake in the Alps, Environ. Microbiol. Rep., 6, 618–624, 2014.

Pöhlker, C., Huffman, J. A., and Pöschl, U.: Autofluorescence of atmospheric bioaerosols – fluorescent biomolecules and potential interferences, Atmos. Meas. Tech., 5, 37–71, https://doi.org/10.5194/amt-5-37-2012, 2012.

Prenni, A. J., Tobo, Y., Garcia, E., DeMott, P. J., Huffman, J. A., McCluskey, C. S., Kreidenweis, S. M., Prenni, J. E., Pöhlker, C., and Pöschl, U.: The impact of rain on ice nuclei populations at a forested site in Colorado, Geophys. Res. Lett., 40, 227–231, https://doi.org/10.1029/2012GL053953, 2013.

Raisi, L., Aleksandropoulou, V., Lazaridis, M., and Katsivela, E.: Size distribution of viable, cultivable, airborne microbes and their relationship to particulate matter concentrations and meteorological conditions in a Mediterranean site, Aerobiologia, 29, 233–248, https://doi.org/10.1007/s10453-012-9276-9, 2013.

Raupach, M. R. and Lu, H.: Representation of land-surface processes in aeolian transport models, Environ. Model. Softw., 19, 93–112, https://doi.org/10.1016/S1364-8152(03)00113-0, 2004.

Robertson, B. and Alexander, M.: Mode of dispersal of the stem-nodulating bacterium, Azorhizobium, Soil Biol. Biochem., 26, 1535–1540, 1994.

Rosselli, R., Fiamma, M., Deligios, M., Pintus, G., Pellizzaro, G., Canu, A., Duce, P., Squartini, A., Muresu, R.,

and Cappuccinelli, P.: Microbial immigration across the Mediterranean via airborne dust, Sci. Rep., 5, 1–10, 16306, https://doi.org/10.1038/srep16306, 2015.

Schlesinger, P., Mamane, Y., and Grishkan, I.: Transport of microorganisms to Israel during Saharan dust events, Aerobiologia, 22, 259–273, https://doi.org/10.1007/s10453-006-9038-7, 2006.

Schwarzbach, E.: A High Throughput Jet Trap for Collecting Mildew Spores on Living Leaves, Journal of Phytopathology, 94, 165–171, https://doi.org/10.1111/j.1439-0434.1979.tb01546.x, 1979.

Scire, J. S., Strimaitis, D. G., and Yamartino, R. J.: A user's guide for the CALPUFF dispersion model, Earth Tech, Inc. Concord, MA, 521 pp., 2000.

Seinfeld, J. H. and Pandis, S. N.: Atmospheric Chemistry and Physics: From Air Pollution to Climate Change, Wiley, 1232 pp., 2012.

Sesartic, A., Lohmann, U., and Storelvmo, T.: Bacteria in the ECHAM5-HAM global climate model, Atmos. Chem. Phys., 12, 8645–8661, https://doi.org/10.5194/acp-12-8645-2012, 2012.

Sesartic, A., Lohmann, U., and Storelvmo, T.: Modelling the impact of fungal spore ice nuclei on clouds and precipitation, Environ. Res. Lett., 8, 014029, https://doi.org/10.1088/1748-9326/8/1/014029, 2013.

Sims, P. L. and Singh, J. S.: The Structure and Function of Ten Western North American Grasslands: II. Intra-Seasonal Dynamics in Primary Producer Compartments, J. Ecol., 66, 547–572, https://doi.org/10.2307/2259151, 1978.

Slinn, W. G. N.: Predictions for particle deposition to vegetative canopies, Atmos. Environ., 16, 1785–1794, https://doi.org/10.1016/0004-6981(82)90271-2, 1982.

Sow, M., Alfaro, S. C., Rajot, J. L., and Marticorena, B.: Size resolved dust emission fluxes measured in Niger during 3 dust storms of the AMMA experiment, Atmos. Chem. Phys., 9, 3881–3891, https://doi.org/10.5194/acp-9-3881-2009, 2009.

Stier, P., Feichter, J., Kinne, S., Kloster, S., Vignati, E., Wilson, J., Ganzeveld, L., Tegen, I., Werner, M., and Balkanski, Y.: The aerosol-climate model ECHAM5-HAM, Atmos. Chem. Phys., 5, 1125–1156, https://doi.org/10.5194/acp-5-1125-2005, 2005.

Szyrmer, W. and Zawadzki, I.: Biogenic and Anthropogenic Sources of Ice-Forming Nuclei: A Review, Bulletin of the American Meteorological Society, 78, 209–228, https://doi.org/10.1175/1520-0477(1997)078<0209:BAASOI>2.0.CO;2, 1997.

Tai, A. P. K., Mickley, L. J., and Jacob, D. J.: Correlations between fine particulate matter ($PM_{2.5}$) and meteorological variables in the United States: Implications for the sensitivity of PM2.5 to climate change, Atmos. Environ., 44, 3976–3984, https://doi.org/10.1016/j.atmosenv.2010.06.060, 2010.

Taylor, N. M., Wagner-Riddle, C., Thurtell, G. W., and Beauchamp, E. G.: Nitric oxide fluxes from an agricultural soil using a flux-gradient method, J. Geophys. Res.-Atmos., 104, 12213–12220, https://doi.org/10.1029/1999JD900181, 1999.

Toprak, E. and Schnaiter, M.: Fluorescent biological aerosol particles measured with the Waveband Integrated Bioaerosol Sensor WIBS-4: laboratory tests combined with a one year field study, Atmos. Chem. Phys., 13, 225–243, https://doi.org/10.5194/acp-13-225-2013, 2013.

Verhulst, P. F.: Notice sur la loi que la population suit dans son accroissement, Curr. Math. Phys., 10, 113–122, 1838.

Waggoner, P.: Removal of Helminthosporium maydis spores by wind, Phytopathology, 63, 1252–1255, 1973.

Waltz, R. A., Morales, J. L., Nocedal, J., and Orban, D.: An interior algorithm for nonlinear optimization that combines line search and trust region steps, Math. Program., 107, 391–408, https://doi.org/10.1007/s10107-004-0560-5, 2006.

Weil, T., De Filippo, C., Albanese, D., Donati, C., Pindo, M., Pavarini, L., Carotenuto, F., Pasqui, M., Poto, L., Gabrieli, J., Barbante, C., Sattler, B., Cavalieri, D., and Miglietta, F.: Legal immigrants: invasion of alien microbial communities during winter occurring desert dust storms, Microbiome, 5, 1–11, https://doi.org/10.1186/s40168-017-0249-7, 2017.

Whitehead, J. D., Gallagher, M. W., Dorsey, J. R., Robinson, N., Gabey, A. M., Coe, H., McFiggans, G., Flynn, M. J., Ryder, J., Nemitz, E., and Davies, F.: Aerosol fluxes and dynamics within and above a tropical rainforest in South-East Asia, Atmos. Chem. Phys., 10, 9369–9382, https://doi.org/10.5194/acp-10-9369-2010, 2010.

Whitman, W. B., Coleman, D. C., and Wiebe, W. J.: Prokaryotes: The unseen majority, P. Natl. Acad. Sci., 95, 6578–6583, 1998.

Wiegand, C. L. and Namken, L. N.: Influences of Plant Moisture Stress, Solar Radiation, and Air Temperature on Cotton Leaf Temperature1, Agronomy Journal, 58, 582–586, https://doi.org/10.2134/agronj1966.00021962005800060009x, 1966.

Wilkinson, D. M., Koumoutsaris, S., Mitchell, E. A. D., and Bey, I.: Modelling the effect of size on the aerial dispersal of microorganisms, J. Biogeogr., 39, 89–97, https://doi.org/10.1111/j.1365-2699.2011.02569.x, 2012.

Wilson, M. and Lindow, S. E.: Inoculum Density-Dependent Mortality and Colonization of the Phyllosphere by Pseudomonas syringae, Appl. Environ. Microbiol., 60, 2232–2237, 1994.

Wiman, B. L. B. and Ågren, G. I.: Aerosol depletion and deposition in forests – A model analysis, Atmos. Environ., 19, 335–347, https://doi.org/10.1016/0004-6981(85)90101-5, 1985.

Yan, W. and Hunt, L. A.: An Equation for Modelling the Temperature Response of Plants using only the Cardinal Temperatures, Ann. Botany, 84, 607–614, https://doi.org/10.1006/anbo.1999.0955, 1999.

Yin, X., Kropff, M. J., McLaren, G., and Visperas, R. M.: A nonlinear model for crop development as a function of temperature, Agr. Forest Meteorol., 77, 1–16, https://doi.org/10.1016/0168-1923(95)02236-Q, 1995.

Zawadowicz, M. A., Froyd, K. D., Murphy, D. M., and Cziczo, D. J.: Improved identification of primary biological aerosol particles using single-particle mass spectrometry, Atmos. Chem. Phys., 17, 7193–7212, https://doi.org/10.5194/acp-17-7193-2017, 2017.